Title: Using the pan-genomic framework for the discovery of genomic islands in the haloarchaeon *Halorubrum ezzemoulense*

Authors: Yutian Feng[1], Danielle Arsenault[1], Artemis S. Louyakis[1], Neta Altman-Price[2], Uri Gophna[2], R. Thane Papke[1], Johann Peter Gogarten[1,3,4]

1: Department of Molecular and Cell Biology, University of Connecticut, Storrs, CT 06268-3125, USA
2: The Shmunis School of Biomedicine and Cancer Research, Faculty of Life Sciences, Tel Aviv University, P.O. Box 39040, 6997801, Tel Aviv, Israel
3: Institute for Systems Genomics, University of Connecticut, Storrs, CT 06268-3125, USA
4: Correspondence to be sent to: Department of Molecular and Cell Biology, University of Connecticut, 91 North Eagleville Rd, Storrs, CT 06268-3125, USA; E-mail: gogarten@uconn.edu.

Keywords: pan-genome, Haloarchaea, islands, homeoalleles

Abstract

In this study, we use pan-genomics to characterize the organized variability from the widely dispersed halophilic archaeal species *Halorubrum ezzemoulense*. We include a multi-regional sampling of newly sequenced, high-quality draft genomes. Using the pan-genome graph of the species, we discover 50 genomic islands which represent rare accessory genetic capabilities available to members of the species. 19 of these islands are likely the remnant of mobile genetic elements and are enriched for genomic dark matter. 10 islands encode for niche adapting solute transporters, with a cosmopolitan but limited distribution throughout the strains. We also observe rearrangements which have led to the insertion/recombination/replacement of mutually exclusive genomic islands in equivalent genome positions ("homeocassettes"). These conflicting islands encode for similar functions, but homologs from islands located between the same core genes exhibit extreme divergence on the amino acid level. Homeocasettes provide variations for a homologous function, which may confer a greater range of adaptability to the species group. We observe some islands that appear geographically restricted; however, we also observe the coexistence of genomes, in a single geographic region, with and without certain genomic islands, demonstrating the retention and spread of rare genes in the pan-genome.

Introduction

Genomic islands (GIs) are loci in a genome that were acquired through horizontal gene transfer. Genes within GIs frequently differ from those in the rest of the genome (Hacker and Carniel, 2001; Juhas et al., 2009) in gene organization, local nucleotide composition and codon usage (Juhas et al., 2009). Acquisition through HGT or recombination is a fundamental part of the GI definition. Compositional differences from the genome's average, the presence of mobility elements and their proximity to tRNA genes are frequently used as surrogate methods, albeit often ineffective (Ragan, 2001; Cortez et al., 2005), to identify GIs in addition to their limited distribution among a group of related organisms (Bertelli et al., 2017; Lu and Leong, 2016). The term "genomic island" is an umbrella term that encompasses different types of islands, including defense, pathogenicity/virulence, and niche adaptation. The typing of a genomic island is determined by the genes encoded on it and the phenotype/capabilities it confers onto the host post-acquisition. Defense islands encode for defense systems such as restriction modification systems, which target foreign DNA, and are active players in the genetic arms race which underlies the evolution of prokaryotic organisms which partake in horizontal gene transfer (Makarova et al., 2011). Pathogenicity islands can fundamentally alter the effect of a microorganism on the disease state of its eukaryotic host (Gal-Mor and Finlay, 2006). Niche adapting genomic islands encode for capabilities which may improve the fitness or survivability of the organism, which harbors it, in response to specific environmental stresses. Genomic islands exhibit diverse origins and functions; based on their persistence, ubiquity, transferability, and encoded functions, they clearly have played decisive roles in the evolution of prokaryotic organisms.

There is no doubt as to the importance of horizontal gene transfer's (HGT or HT: horizontal transfer) impact on evolution (Daubin and Szöllősi, 2016; Gogarten et al., 2002). The successful transfer of a functional gene between two extant organisms may instantaneously provide the recipient with novel traits bypassing the drawn-out adaptation of a gene already present in the genome through mutations. This utility extends to genomic islands, as they encompass a set of interacting genes which may encode for a related function (i.e., HGT "en-masse"). The transferability of genomic islands is reflected by their limited distribution in unrelated genomes, as well as the enrichment of transposases, conjugation related genes and integrases in or around the immediate gene neighborhood of genomic islands (Bertelli et al., 2017; Clasen et al., 2018; Gauthier et al., 2022).

The Haloarchaea are one of the best known and well sampled groups of Archaea. Their obligate halophily (often in environments with salt concentration above 2.0M NaCl) (Bardavid and Oren, 2012; Oren, 2008), selective phototrophy (Sharma et al., 2007), and metabolic capabilities are well documented. In addition to halophily, the genome content of Haloarchaea reflects environmental pressures like limited nutrient availability, prolonged exposure to UV radiation, and the genetic arms race with selfish genetic elements and viruses. Haloarchaea are well-known for their ability to exchange DNA within and between species and even across domains (Huang and Gogarten, 2006; Naor et al., 2016; Williams et al., 2012). Haloarchaeal species frequently undergo homologous recombination, facilitating the spread of alleles and genes within local populations (de la Haba et al., 2018; Makkay et al., 2020; Papke et al., 2015; Soucy et al., 2014; Williams et al., 2012). These characteristics pave the way for the acquisition (from outside the species), and transfer of loci between closely related genomes.

To investigate the gene content and diversity of genomic islands in Haloarchaea, we focused on a single species, *Halorubrum ezzemoulense* (*Hez*). This species was first described in 2006 based on a single strain cultivated from an Algerian sabkha (Kharroub et al., 2006). Later, with more cultivated strains, *Hez* was evaluated using a polyphasic approach (de la Haba et al., 2018) and the species was expanded and eventually amended to include *Halorubrum chaoviator* strains (Corral et al., 2018). Standard experimental DNA-DNA hybridization (DDH) values of *Hez* were correlated to their 16S rRNA and multi-locus gene sequence divergences (de la Haba et al., 2018). In each case, the 70% DDH cut-off corresponded to >99 % nucleotide sequence identity for all the genes analyzed in their sample. We assembled a dataset consisting of 47 sequenced isolates of *Halorubrum ezzemoulense*, 37 of which were newly sequenced and assembled into draft genomes for this study (see data availability section for the genome files and Spreadsheet S1 for genome information). Every genome of our current dataset is a member of the same species, having at least 98.5% pairwise average nucleotide identity, though most of the strains share above 99% identity (Supplemental Spreadsheet S2). These strains were isolated from various geographic locations, including but not limited to: Santa Pola Saltern (Spain), Aran-Bidgol (Iran), and the Dead Sea (Israel). Limiting the dataset to members of the same species informs on what kind of rare/flexible gene content is maintained and diversified in that group.

We report the distribution and content of 50 GIs with a limited distribution within the *Hez* species, discovered using the pan-genome graph approach described in Panaroo (Tonkin-Hill et al., 2020). 10 of these islands contain the components of solute transporters, demonstrating differential metabolic capabilities within members of the same species. We also find that GIs often are found inserted between the same core genes as other islands and, furthermore, encoding for related functions in a mutually exclusive fashion. We dubbed these matching islands "homeocassettes". Although inserted between the same core genes and encoding in part homologous genes, these homeocassettes exhibit extreme divergence and are the result of extensive duplication and reassortment events.

Results and Discussion

Hez pan-genome reveals flexible gene content

Using the Panaroo pipeline, we used sequence identity and local synteny to cluster the predicted genes throughout all 47 *Hez* genomes into pan-gene families. When available, pan-gene families were named according to their annotations' consistency throughout all the genomes, otherwise pan-gene families were named by arbitrary ascending group numbers. The entire genetic repertoire or "pan-genome" of *Hez* consists of 8,401 pan-genes. The core genome, or those genes found in at least 95% (44) of all *Hez* draft genomes, includes 2,621 pan-gene families (Fig S1). Given the average *Hez* genome contains ~3,500 genes, a core division of this size reflects not only the essential/housekeeping genes but also *Hez* lineage specific genes. The shell genome, here defined as non-core genes identified in at least 2 genomes, is the largest fraction of

the pan-genome (4,072 pan-genes). This suggests that rare genes (non-core genes) are shared between members of the species. This may be a consequence of different genetic specializations/mosaicism present in the species and/or reflect predation by mobile genetic elements. Pan-genome accumulation and core-genome rarefaction curves, as well as a description of each pan-genome division is found in Supplemental Fig S1. Detailed information of the 47 *Hez* genomes including assembly statistics, number of unique pan-genes, and secondary replicon information is included in Supplemental Spreadsheet S1. These pan-genome inferences reveal a flexible genome content, and produced a gene-connectivity graph which was used to discover and elucidate the local context of 50 pan-genomic islands.

Isolates Overview

Pairwise comparisons of average nucleotide identity (ANI) and genome alignment fraction, following methods by Gosselin et al., 2022 (Gosselin et al., 2022), confirm that all 47 strains are of the same species (Supplemental Spreadsheet S2). The phylogeny based on corrected tANI data (Fig 1) reveals regionally delimited clans (highlighted clans from Spain and Israel in Fig 1), and well-supported groups formed by isolates from multiple regions. Isolates from Spain and Israel not placed within the regionally delimited groups (Fig 1, highlighted clades) cluster with isolates from other regions. The tANI phylogeny reflects both, sequence variation in the core genome and the flexible gene content across all genomes. Another phylogeny (Supp. Fig S2), based only on core genome differences, was inferred using a nucleotide concatenate of all 2,621 core genes (where ~2.2M of 2.3M sites were constant). Both phylogenies recover a similar topology including both regionally delimited groups, but strains not associated with a group were placed differently due to shared accessory genes. For example, strain UG96 shares several genomic islands with other Israeli isolates (Island 1, 4, 23, etc.; Fig 2), and is placed with the Israeli isolates in the tANI phylogeny but is placed outside this group with respect to the core genes. This observation is consistent with the notion that flexible genome content, such as the genes encoded on genomic islands, impact placement of groups in the tANI phylogeny (Fig 1).

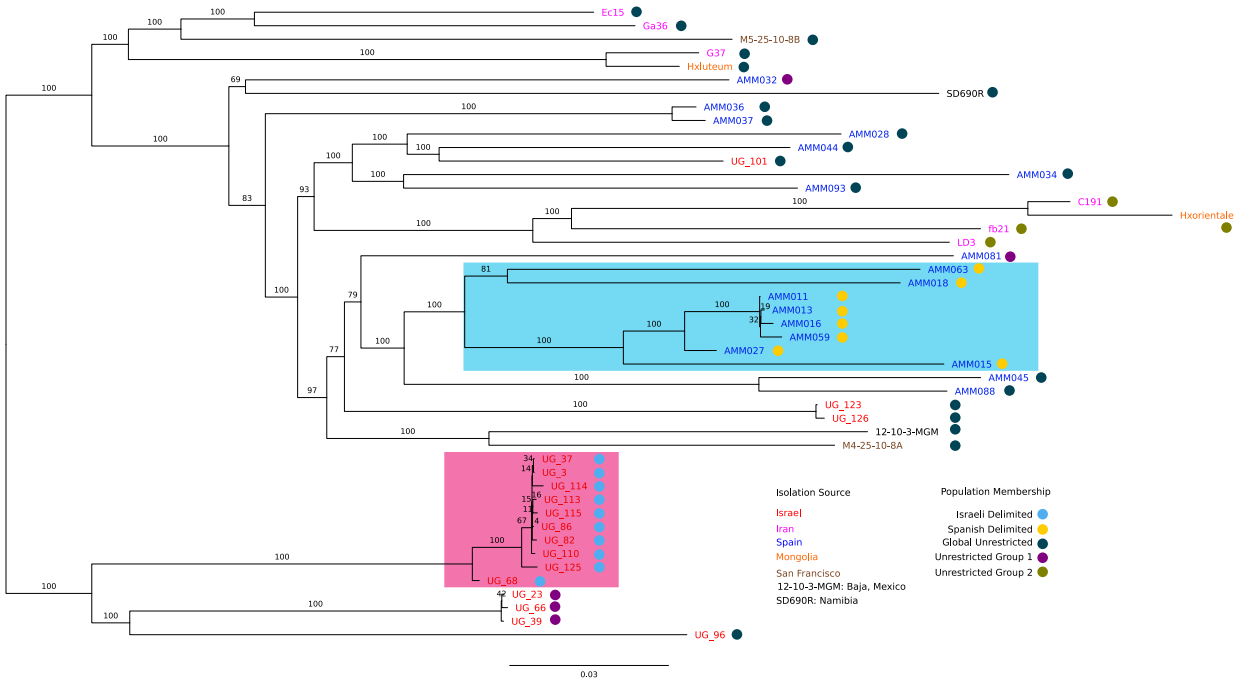

Figure 1. **Overview of Hez strain phylogeny and nested population structure.** The phylogeny was calculated using pairwise ANI and genome alignment fraction, as well as bootstrapped following the methods of Gosselin et al., 2022. A distance matrix showing all the pairwise relationships can be found in Supplemental Spreadsheet S2. Branch supports are denoted by the numbers above the branches. The coloring of the tip labels indicates isolation region. Each strain has been assigned membership into nested populations using rhierBAPs, which is designated by the colored circle at each tip. The highlighted clades indicate that the population membership (reflecting core genome) and phylogenetic grouping (reflecting whole genome) both agree that these are regionally delimited clans in Spain (cyan) and Israel (pink).

In addition to phylogenies, we performed hierarchical clustering of isolates using rHierBAPs (Tonkin-Hill et al., 2018) (which is based on SNPs found in neutral core genes), this inference revealed a nested population structure within *Hez* (Fig 1; population membership shown with circle indicators). The regionally delimited clans in Spain and Israel observed in the tANI phylogeny correspond to nested population structures when analyzing the SNPs of neutral core genes (Fig 1, highlighted clans). This may reflect potential barriers to dispersal and recombination in these regions. These regionally delimited groups (Fig 1: blue circles [Israel] and gold circles [Spain]) may represent lineages diverging within the overall Hez species. The inferred populations, excluding those confined to a single clade (purple, dark blue, and olive circles), indicate information exchange or migration at a global scale. The largest population, represented by the dark blue circle (Global), encompasses SNP contributions from strains in every isolation location and spans almost every group in the phylogeny. This may reflect either an ancestral lineage of *Hez* or a cosmopolitan strain with little barriers to recombination.

Islands in the Hez pan-genome

The Panaroo pipeline produces a pan-genome graph (Tonkin-Hill et al., 2020), that represents gene families and their connectivity in each genome. The pan-genome graph is analogous to a De Bruijn assembly graph, where the nodes are gene families instead of contigs, and the edges describe the gene adjacency information for each gene family (see Fig 3). Node by node traversal of this pan-genome graph, considering the genome representation at each node (i.e., a core gene has a representation = 47 and a unique gene = 1), returns the pan-genomic islands that have been integrated in between core genes (see methods "Querying the Pan-genomic Graph"). By employing this pan-genome graph-based approach, larger scale gene transfers can be reliably detected even when the local gene neighborhood is confounded with gene acquisition/loss, structural rearrangements, and poor quality of the draft genome assembly. Reliability in this case stems from the requisite of core genes flanking the island, as the local gene neighborhood and representation of the core genes must be recovered from at least 44 of 47 *Hez* genomes. This is analogous to the approach which identifies genomic islands as low coverage regions when metagenomic reads are mapped onto an isolate's genome (Coleman et al., 2006; Tschitschko et al., 2018). The pan-genome graph resembles the reference genome, while individual genomes act as metagenomic reads. The sharp drop from high coverage spanning core genes to pan-genomic islands with low coverage illustrates the flexibility of gene content. We note that only genomic islands found in the cloud or shell will be discovered using this approach and we only considered pan-genomic islands which encode at least two genes (although islands of size one were included when they were found to invade the same core genes as another island; see below "homeocassettes").

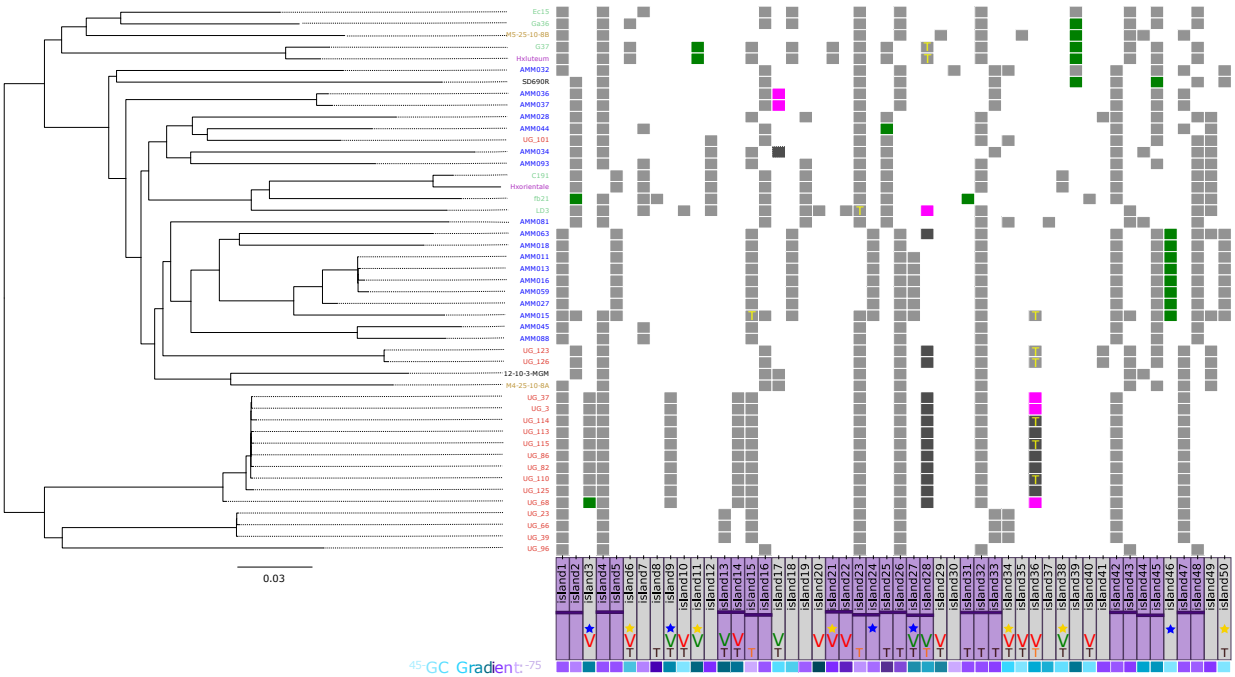

Figure 2. **Heatmap distribution of genomic islands in *Halorubrum ezzemoulense*.** The presence/absence heat-map of discovered pan-genomic islands (x-axis) mapped onto the tANI phylogeny. The y-axis are the genomes in which the islands are present, the tip labels are colored based on the region of isolation (red: Dead Sea, Israel; blue: Santa Pola, Spain; brown: San Francisco, USA; green: Iran; purple, Mongolia; SD690R: Namibia; and 12-10-3-MGM: Baja California, Mexico). The purple boxes indicate conflicting genomic islands, islands invading the same core genes have a purple horizontal dash spanning adjacent purple boxes, at the same height. Below the island names is an indication of average G+C% for coding sequences found on the island. A blue star beneath the island name indicates that the island sequences are identical in the genomes that have it (*i.e.*, Island 27's sequence is identical across the Spanish strains which have it). Similarly, a yellow star indicates that the sequences of that island are identical, and the island is found in multiple geographic regions (and coexists in those regions with isolates without the island). A red **V** under the island name indicates that the island encodes an integrase, while a green **V** indicates that there are restriction modification system components in addition to encoding the integrase. The presence of a black "T" under the island name indicates that tRNAs flank the genomic island in all genomes. While an orange "T" means that a flanking tRNA is found in a small portion of the genomes and these genomes are indicated with the "T" inside of their corresponding box. Green boxes on the heat-map indicate that a transposase (IS element) was found in the genomic neighborhood (±5 genes) of the island, in that genome. Exact family designations and names of transposases can be found in Supplemental Spreadsheet S7. Magenta boxes indicate that a flanking transposase was found but the ORFs on the genomic island have been shuffled or that the island is only a partial representation of the full genomic island found in other genomes. Similarly, dark gray boxes show the partial genomic island without the presence of a flanking transposase.

Analysis of the pan-genome graph reveals 50 distinct pan-genomic islands in the *Hez* genomic repertoire (Fig 2). These islands encode diverse functions and unannotated hypothetical proteins, making comprehensive annotation challenging. The functional description of all the islands, their encoded genes, and adjacent core genes is listed in Supplemental Spreadsheet S3. Some islands exhibit preferred geographic distributions corresponding to regionally delimited groups and populations from Spain and Israel (Fig 1). Specific islands, like 3, 9, 13+14, are exclusively found in the Israel clade, indicating divergence and accumulation of rare genes in these regionally restricted groups. Islands 6, 18, 24, 27, 46, and 50 are predominantly found in Spanish strains but occur rarely in other regions. In the case of Islands 15 + 16, which invade between the same core genes, regionally restricted groups (from both Spain and Israel) only have Island 15, while the other genomes spanning multiple regions and populations have Island 16 instead. For several islands we identified putative functions or conserved domains (Islands 4, 5, 7, 15, 18, 24, 31-33, and 44-47) such as: von Willebrand Factor type A domains, intracellular signaling, and sulfur metabolism (see Supp. Spreadsheet S3 for full descriptions). The distribution among isolates suggests that these islands play roles in the specialization and niche adaptation of different *Hez* strains.

Mobile islands encode ensembles of hypothetical proteins

Notably, 19 islands contained integrases; these islands are denoted in Fig 2 by a red or green V and summarized in Supp. Spreadsheets S3,4. Most of these islands displayed distinct G+C content (40-55%, all but Islands 21+22) compared to the average of the core genome (~68%). While these islands encode recombinases or integrases, these genes are accompanied by ensembles of hypothetical proteins, for which annotations are unavailable. This is unsurprising as mobile genetic elements encode many unannotated proteins due to their propensity for mobility and fast evolution (Peck and Lauring, 2018; Martínez-García et al., 2014). We used geNomad (Camargo et al., 2023) to identify and classify the viruses and plasmids present in each genome assembly. Only Islands 36 and 38 were classified as viruses or plasmids. The absence of viral/plasmid hallmark proteins on the other islands suggests that they may not be actively replicating as a separate entity from the chromosome and represent remnants of integrated mobile genetic elements. The G+C deviation, rarity throughout the pan-genome, and enrichment for uncharacterized genes are attributes these integrase containing islands share.

Six of these islands encoded genes for defense systems against foreign DNA in the form of restriction modification system (RMS) genes. Of the 94 RMS-related genes in the entire *Hez* pan-genome, 10 were found on islands (a heatmap summarizing this distribution can be found in Fig S3). RMS encoding islands are rare, each observed in only 2-10 genomes (Supplemental Spreadsheet S5). Island-encoded RMS genes exclusively occurred on integrase-containing islands suggesting selection for transmissibility and evasion of resistance mechanisms. Transmissibility is a means to circumvent resistance mechanisms innovated by other mobile genetic elements, that may have been the target of these RMS genes. The Supplemental Discussion includes a more detailed discussion of RMS systems.

Transferability of flexible gene content encoded on pan-genomic islands

While many islands have diverged and accumulated genome specific mutations, 11 islands have an identical nucleotide sequence across the genomes they are found in (Fig. 2). In all cases, except Island 38, these identical islands are found in different geographical regions, different clans, and have a limited distribution amongst isolates from the same region. The sequence of Island 11, for an example, is found identically in genomes from Mongolia, Spain, Israel, and Iran. However, the island is still rare in those regions with only 1-2 genomes per location having acquired it. The coexistence of strains with and without the island in the same environment demonstrates the flexibility of that locus. When islands with limited distribution are found across different geographic regions, with an identical sequence, horizontal transfer and migration are plausible explanations for their distribution. We inferred the number of duplications, transfer, and loss (DTL)

events for all 50 genomic islands and core genes (2518 total) via topological reconciliation of gene and the species tree (Fig 1) using RangerDTL (Bansal et al., 2018). Genes on a genomic island were concatenated to build an island tree. The genomic islands were inferred as transferred and lost significantly more frequently (two-sided T-test $p < 0.01$) compared to core genes. After normalization, the average transfer events inferred in the genomic islands was 0.23 (events / (internode x total branch length), while it was 0.15 (events / (internode x total branch length) for core genes. In addition, there were significantly more gene loss events ($p < 0.001$) in genomic island trees as compared to core genes. The full report of DTL events inferred for every gene tree can be found in the Supplemental Spreadsheet S6. While we can infer DTL events for those islands where tree building is possible (i.e., there are at least 3 taxa and the sequences are not identical), the presence of doubleton islands also are likely the result of a transfer if the island is found across multiple geographic regions or phylogenetic groups (e.g., Island 10, 38).

The loci containing these pan-genomic islands are enriched in mobilizing genetic elements. After island discovery, the invasion point (or the immediate two core genes) was expanded to include the genomic neighborhood ±5 genes upstream and downstream of the island. The distribution of tRNAs (T), transposases and integrases in these expanded gene neighborhoods is mapped in Fig 2. In addition, information about transposase families near the islands are included in Supplemental Spreadsheet S7. The propensity of tRNA to form hairpin loops paves the way for the integration of mobile genetic elements (Williams, 2002) and horizontal transfer in *Hez*. While there are 70 total tRNAs encoding genes in the genome of *Hez* (Feng et al., 2019), 18 of them are proximal to these genomic islands. The discovered genomic islands encode a total for 351 genes, or only 9.5% of ORFs, while ~25% of all tRNAs in the genome are in the 5 gene neighborhood of an island insertion point, while not being found on the island itself.

<u>Homeocassettes serve as reservoirs of genetic and gene content variation</u>

Several pan-genomic islands are found between the same core genes, in different genomes, while maintaining local synteny (Fig 2, adjacent purple lines of the same height show same core gene invasion; Supplemental Spreadsheet S8 lists these core genes and their predicted functions). The presence of island pairs is mutually exclusive, meaning that, if one genome has island 1, it does not have island 2, except for strain: AMM015 (see Supplemental Discussion). These island pairs reflect cassette-level variation in the *Hez* pan-genome. The combined genome representation in every island pair (except islands 13+14 [which is restricted to Israeli strains] and island 44+45), is consistent with the distribution of a core gene (present in all genomes). Most of these island pairs (e.g., island 1 and island 2) are ascribed similar functions and share homologs, but the homologous ORFs on conflicting islands are dissimilar enough (in terms of sequence identity and gene neighborhood) to escape clustering into the homologous gene family on the opposing island.

We considered every pairwise combination of genes on each conflicting island pair (where there was not a large difference in the number of ORFs encoded within the set) with blastn, blastp, and PRSS searches (Supplemental Spreadsheet S8). Genes on one island which have homolog(s) on the opposing island were termed "homeoalleles", while genes that do not have homologs on an opposing island were termed "iORFans" (as in "island encoded orphan gene"). Homeoalleles, not to be confused with homeologs in eukaryotes (i.e., a homolog resulting from allopolyploidy), are divergent isofunctional variations of a gene that may be swapped/transferred within an exchange group often in equivalent genomic positions (Andam et al., 2010; Andam and Gogarten, 2011). In Islands 4+5, we observed an instance of within island recombination where a peptidase from Island 5 was swapped with its homeoallele on Island 4 in the strains C191 and Hxorientale (Fig S4), while the other 10 strains which have Island 5 retained the original peptidase. Thus, we term conflicting genomic islands which share homeoalleles as "homeocassettes". We defined homeocassettes as any two conflicting islands which have at least 50% of their gene content as homeoalleles. This somewhat

arbitrary threshold allows the distinction between conflicting islands which share many homeoalleles (Fig 3ab) and those that are likely viral remnants which only share the integrase gene (Fig 3c).

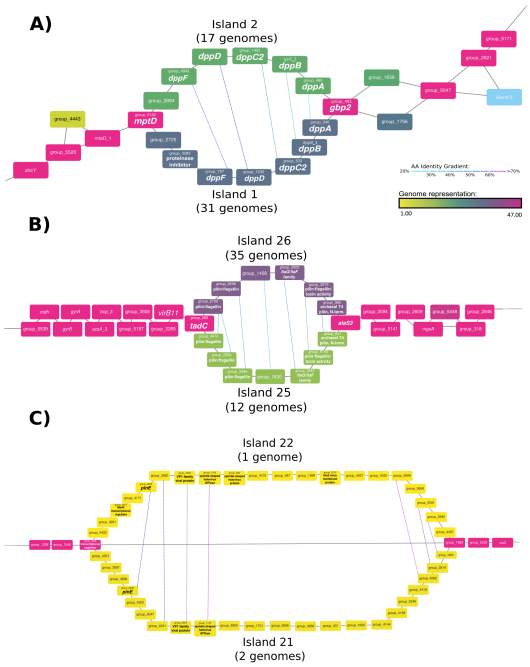

Figure 3. **Pan-genome graph depiction of competitive islands.** Close-ups of several regions of interest in the overall pan-genome graph, which show two pan-genomic islands occupying the same locus. Nodes in each graph represent pan-gene families, while edges indicate contiguity between nodes. Core genes are colored magenta and are represented in at least 44 of 47 isolate genomes. Islands in between the same core genes are mutually exclusive, and dashed lines between genes on opposing islands indicate homology (coloring indicates % identity). When annotations for pan-genes are available they were written inside the node in the larger font, otherwise arbitrary group_names were assigned. A) Both islands encode the components of a putative oligopeptide ABC transporter, *dppABCDF*. Both islands are inserted between the same core genes (*gbp2* and *mptD*) and display mutual exclusivity barring the AMM015 strain (which increases the total genome number to 48). Genes which do not have homologs on the opposing island: group_2884 (island 2), and group_2725 and group_3285 (island 1), reflect the gene content variation which exists across these islands. These two islands are considered a homeocassette. B) These islands encode for a Type 4 pilus system and insert between the ATPase tadC and an alanyl-tRNA ligase. Homologs were found for every encoded gene on opposing islands, and in one case a gene from Island 26 (group_2789) was duplicated on Island 25. Though homologous, these island-encoded genes share low amino acid identity. C) These rare islands insert into the core genes group_3359 (transcriptional regulator) and group_1682. Note the edge which directly connects these two core genes and skips both islands entirely, this indicates that in 44 genomes both islands are not present. Only a small fraction of these island genes has available annotations. Seven genes have detectable homologs across both islands, indicated by the colored dashed lines. Both islands seem to have indications of viral origins (seen in the shared integrase, Vp1, and haloviral proteins), and have a G+C content ~50% (while the core genome has a G+C ~68%). These islands demonstrate genetic and gene content variation captured on islands, and the ability of different islands to insert into the same core genes.

In total, we identified 9 island pairs (18 islands total; Figs 3, S4-9) which have similar or identical ascribed functions (Table 1). Six island pairs were enriched in homeoalleles, forming homeocassettes, while three pairs had more iORFans and shared at least an integrase/recombinase with the opposing island. Opposing islands of a homeocassette were found across geographies and phylogenetic groups (Fig 2). For example, Israeli and Spanish strains have a mixture of island 1 and island 2 within each geographic location. The coexistence of both homeocassettes in the same geographic region suggests the gene content on these islands is maintained rather than outright lost.

Table 1. Summary of Conflicting Island Pairs.

Island Pair	Predicted Function	Invaded core genes	ORFs encoded	# of homeoalleles	Avg. G+C
1+2	Peptide ABC transport.	*gbp2* | *mptD*	7 vs 6	5	65.4%
4+5	Adhesion/signaling	Peptidase S24 | group_5156	7 vs 6	7 (duplication)	68.2%
23+24	Intracellular signaling	*rpaP1* | *acaB1*	3 vs 3	2	70.5%
25+26	Secretion effectors	T2 Sec. System | *alaS*	7 vs 6	7 (duplication)	65.3%
42+43	K^+ ABC transporter	*trkH* | *mmcA*	3 vs 5	4 (duplication)	69.5%
44+45	Unknown (peptidase)	*carB* | *nosL*	6 vs 12	11 (duplication)	57.5%
13+14	Restriction modification	*ribK*| group_4555	10 vs 8	1	55.3%
21+22	Unknown	group_3359 | group_1682	22 vs 20	7	64.5%
27+28	Viral remnant	*fabG* | group_5345	14 vs 12	1	51.3%

Predicted functions of entire islands are estimated based on annotations of encoded ORFs via EggNogMapper (Huerta-Cepas et al., 2019). Islands are classified as unknown if annotations are unavailable. Invaded core genes are reported by their annotations, or otherwise assigned an arbitrary group number if annotation is unavailable. Homeoalleles are reported as 1 unit if a homolog exists on both islands, in the case of an unbalanced duplication another count is added, and this is noted in the parentheses.

Homeocassettes encode diverse functions, and each island within a pair offers a different variation upon that function. They also display exclusive genetic variation and selective organization of gene cassettes/operons for a set of homologs. The observation that homeocassette pairs are located between the same core genes, appears to reflect their integration through homologous recombination in the conserved flanking region following genetic transfer or mating (Naor et al., 2012). The homeocassette pairs we observed in the *Hez* genomes differ in the number of encoded ORFs (Fig 3, Table 1); this difference is due to iORFans or paralogues found on either island. The presence of multiple, presumably synergistic genes or operons on the islands allows the host to gain entire functions with the acquisition of an island. Due to the amino acid sequence divergence displayed by homeocassettes it may be improper to consider them iso-functional *in toto*. Similar to homeoalleles of aminoacyl tRNA synthetases (Andam et al., 2011), the main function of a homeoallele pair may be the same; however, it is likely that the pair differs in some respects that impact organismal fitness under some environmental conditions, which would ultimately affect the persistence and spread of the islands within the population.

The retention of homologous, but highly divergent GIs in equivalent genome positions may facilitate the adaptation to specific environmental niches. The islands might encode weakly selected functions *sensu* Lawrence and Roth (Lawrence and Roth, 1996), and this would have contributed to their faster divergence compared to the core genes. However, the divergence between the contained homeoalleles on paired homeocassettes is so great that we conclude that the divergence of the homeocassettes preceded the divergence of the studied *Hez* strains by many orders of magnitude. Different variants of the same gene

cassette may offer unique advantages in different conditions, especially if the environment is heterogenous. Those islands which encode surface components (such as Islands 1+2, 4+5; see Spreadsheet S3) are also likely to be virus receptors. Multiple viral receptors in a single meta-population may confer immunity to predators in a sub-population. The co-occurrence of homeocassette pairs in the same region (in different genomes) and the swap of endopeptidase homeoalleles observed in Islands 4+5 (in strains C191 and Hxorientale; Fig S4), indicates that it is possible for an organism to switch between the contents of a pair through recombination of the conserved surrounding regions. It is also possible that homeocasettes may play a role in speciation by acting as the crystallization points for expanding regions of divergence where barriers to within group recombination are erected.

Differential solute transporter utilization amongst *Hez* isolates

10 of the islands encode the components for various transporters: 8 ABC transporters and 2 trk-type transporters (Supplemental Spreadsheet S9). These transporter islands (Supp. Spreadsheet S9) have an average G+C which closely resembles the *Hez* core genome. In contrast to islands which encode integrases, almost every gene on transporter islands could be annotated. Furthermore, transporter islands have high genome representation, suggesting the genes encoded on them have greater utility and therefore higher lineage persistence than genes found on integrase encoding islands. Transporter encoding islands illustrate the utility of the pan-genome graph for GI discovery, as they do not display obvious organizational deviations from the genome average. These islands are not the result of HGT from outside *Hez*, and seem to have evolved, recombined, and spread within *Hez* and earlier related lineages. The limited distribution displayed by transporter islands reflects differential availability or utilization of environmental solutes amongst members of *Hez*, otherwise the transporters would be completely fixed or lost in the population. These discovered transporters have putatively ascribed substrates which include reduced carbon compounds, phosphate, polyamines, small peptides and potassium ions. The physiological and evolutionary implications of these transporter islands are discussed in extensive detail in the Supplementary Discussion.

Island 19 is the sole instance of a complete carbohydrate uptake transporter (CUT) in the *Hez* pan-genome, found in a few Iranian, Mongolian, and Spanish strains (6 total), but notably absent in Israeli isolates. The presence of homologs to genes from the two described CUT operons from *Pyrococcus furiosus* (Lee et al., 2007), suggests its ability to import both trehalose/maltose and maltodextrin. Strains which harbor this island have a greater range of nutritional competence when those carbohydrates are present in the environment.

Polyamines (such as agmatin) reportedly play crucial roles in Archaea, modifying translation factors and tRNA, which are essential for translation (Hamana et al., 1985; Kamekura et al., 1986; Prunetti et al., 2016). Earlier studies noted the complete absence of polyamine biosynthesis genes in Haloarchaea (Chen and Martynowicz, 1984). Later studies reported the discovery of agmatinase (*speB*) but noted the lack of a polyamine import mechanism for which *speB* would act in concert (Prunetti et al., 2016). Island 16 is a sporadic island which encodes 5 genes for polyamine import (*potABCD* system (Kashiwagi et al., 2002)). This presents a possible polyamine scavenging system which confers a growth advantage for those strains which have acquired Island 16 (Fig 2) in environments where polyamines are present.

Islands 42+43 in *Hez* are homeocassettes that encode TrkAH transporters (Fig S8). Unlike other transporter islands, these TrkAH transporters are not energized by ATP hydrolysis (Harms et al., 2001). K+ import plays a critical role for the salt-in strategy employed by *Hez* and other Haloarchaea (Mongodin et al., 2005). Island 43 stands out as it contains a variant of the *trkA* core gene found upstream of the homeocasette insertion point (Fig S8). The core TrkA has 480 amino acids, while the island-encoded TrkA is shorter, consisting of 230 amino acids and displays high similarity to the N-terminal portion of the core TrkA. Previously, a similar truncated *trkA* gene in *Thermotoga maritima* was considered a pseudogene due to a frameshift mutation (Johnson et al., 2009; Nelson et al., 1999). However, complementation assays (Johnson et

al., 2009) revealed that these truncated TrkA proteins, along with a novel membrane-spanning protein, form a new sub-class of K+ importers known as the two-subunit TrkA importer (more in Supplemental Discussion). The existence of Islands 42+43, and the core TrkAH genes highlights the diverse potassium import strategies present in the *Hez* pan-genome (Fig S8).

5 of the transporter islands encode divergent (up to 50% amino acid identity) putative di/oligopeptide transporters (*dppABCDF* operon), including two homeocasette pairs (Fig 3a). The core genes of these 5 islands include the necessary components of an ABC transporter which traffics small peptides, however, the ATP coupling proteins DppD+F are fused into one ORF on Island 12 (Fig S10). Accessory genes on these islands (i.e., those genes not homologous to the ABC transporter components) are involved in amino acid metabolism, suggesting these islands genuinely import peptides. Strains with Island 39 demonstrate flexibility in its classification as a plasmid or integrated into the chromosome. These findings are consistent with the notion that pan-genomic islands act as reservoirs of genetic variation, allowing the retention of divergent gene cassettes over time. These differences between the islands suggest each island has diverged to accommodate slightly different peptide substrates. Consequently, different strains of *Hez* can adapt to different peptide availabilities in different environments and have a greater range of niche adaptability.

Island encoded phosphate transporter is a variation of a homologous core gene neighborhood

Island 49 encodes a variant of the *phnCDE* operon, which was experimentally associated with eDNA uptake in conditions where phosphorous was a limiting nutrient in *Haloferax volcanii* (Pearson, 2022). This GI was found in 15 genomes across different geographic regions. A homologous, but divergent *phnCDE* gene cluster was also found in the *Hez* core genome over 2.36M bp downstream of the island insertion point (Fig S11). The *Hez* core-*phnCDE* cluster displays greater similarity to the *Haloferax volcanii* phnCDE system in which the knockout experiments were performed. Island 49 encodes not only the *phnCDE* homologs, but also contains a duplicated permease (*phnE2*) and a HAD hydrolase which affirms the island's association with phosphate/phosphonate import (see the Supplemental Discussion). The island encoded *phnE1* and *phnE2* genes are also present in *Haloferax volcanii,* where they are encoded on the megaplasmid pHV4, but this gene neighborhood does not contain homologs of the *phnCD* genes (Fig S11).

The presence of two homologous phosphate uptake systems in *Hez* demonstrates the role of pan-genomic islands in diversity generation. Many of these islands and homeocassettes contain the result of an unbalanced gene duplication (Supplemental Spreadsheet S8, the duplications are highlighted in yellow). Many of these duplications are not ancestral, as these islands have a sporadic distribution across regions and phylogenetic groups (Fig 2). In this work, duplicated genes tend to reassociate with homologous, but divergent variants of genes possibly recombined from the source gene neighborhood, this is seen in several of the illustrated examples (Island 49: Fig S11, Islands 4+5: Fig3b, Islands 25+26: Fig3b). The fate of duplicated genes is often neofunctionalization or pseudogenization, in the case of *phnCDE* system on Island 49 the former seems to be the case. This is because homologs of the *phnCD* genes are also found on the same island. While the acquisition or duplication of a core gene may seem wasteful and counter-productive to fitness (redundant genes and energetic costs), it may be the starting point of genetic divergence or lead to greater niche adaptability in the species. Retchless and Lawrence (Lawrence and Retchless, 2010) showed that the acquisition of an adaptive gene can be the starting point of genome divergence spreading out from this gene into the gene's neighborhood. This acquisition event is not dissimilar to a gene duplication into a distant locus, as seen in Island 49. The reconstitution of homologous genes from the source gene neighborhood in the duplicated gene neighborhood illustrates the selective/selfish manner with which gene neighborhoods form. The duplicated gene has a greater chance of persistence and replication if it can be transferred and utilized in synergy with the other homologous components of the same system.

Conclusion

Using a pan-genomic framework, namely the pan-genome graph, for the discovery of islands has a few advantages. Principally, this method allows for the detection of islands that have the same underlying architecture (GC content, gene density, etc.) as the genome of the host. Discovery of genomic islands using the pan-genome graph does not rely on a reference genome and is extensible to any dataset containing highly related (and syntenic) genomes. Homeocassettes and those islands encoding ABC transporters would not be detected with a method that focuses on deviations from host architecture. Additionally, a measure of reliability and support can be attributed to islands found under this framework. All the islands must be syntenic, or the graph pathing will fork and create singleton islands that would corrupt or complicate (Fig. S7, S9) the order of genes. This graph-based framework allows for the exploration of gene neighborhood surrounding the island, in all the included genomes, which can uncover mobilizing elements that may explain the ontology of the island.

Broadly, there seems to be few barriers to horizontal transfer between strains of *Halorubrum ezzemoulense* in distant geographic locales, although strains in the regionally delimited groups (Fig 1; highlighted clades) share more GIs with each other than with those strains outside the groups. Pan-genomic islands play an important role in the generation and upkeep of within species variability and persist as divergent units even if two islands occupy the same locus. The discovered transporter islands provide a greater range of niche adaptability, while not changing the fundamental genetics of a species member. Rare island encoded genes are made accessible to other species members via recombination using the conserved surrounding regions as a template. Some genomic islands, however, harbor or are the remnants of selfish genetic elements, which take advantage of *Hez's* propensity for recombination to persist and spread to new uninvaded populations. These findings illustrate how islands confer genetic and gene content variation to *Hez*.

Methods

Isolates collection, sequencing, and genome assembly

Spanish isolates were collected and sequenced using the methods described in (Feng et al., 2019), while Israeli isolates' protocol resembled the sampling methods described in (Feng et al., 2021). Reads were assembled with SPAdesv3.11.1, on default parameters using 150 bp reads. The genome of *Hez* strain fb21 was assembled using a combination of short and long Pac-Bio reads, as described in Feng et al., 2019. Genomes were also mined from NCBI to supplement the in-house isolates; their accession numbers are provided in Supplemental Spreadsheet S2. Genome assembly quality was assessed with CheckMv1.0.7 (Parks et al., 2015), using the 149 Archaeal marker set. Genomes with low completeness and high contamination were discarded, the genomes quality report is shown in Supplemental Spreadsheet S2. In addition, the qualities of the genomes were processed by the panaroo-qc script (Tonkin-Hill et al., 2020), and additional outlying genomes were removed.

Genome distance calculation and tANI phylogeny

Genome distance was calculated using an extension of the jANI algorithm (Gosselin et al., 2021.), which also takes into account the alignment fraction (AF) of the genomes. The genome distances were used to construct a phylogenetic tree, with bootstrap support per the tANI method. Genomes with a distance <0.315 (with AF =1, this corresponds to ANI >73%) are considered members of the same species. The complete distance matrix is displayed in Supplemental Spreadsheet S1,the resulting phylogeny is depicted in Figure 1.

Gene calling, gene family clustering, and pan-genome graph generation

ORFs were predicted and annotated in these genomes using Prokkav1.14 (Seemann, 2014), under the same gene model (trained for *Hez* genomes), under the default settings and with the Archaea flag. In addition, all gene families were cross annotated with EggNOG-Mapper5 (Huerta-Cepas et al., 2019), and several genes of interest were predicted in HHPred (Zimmermann et al., 2018). Predicted ORFs were clustered into gene families using multiple steps: 1) identity threshold (98%), and 2) graph-based-clustering where gene families from different genomes are collapsed into the same family if their local synteny is conserved throughout multiple corrections and filtering of the graph, as described in Tonkin-Hill, et al., 2020 (Tonkin-Hill et al., 2020). The resulting clustered gene family nucleotide sequences were aligned with MAFFT (atoh and Standley, 2013), and their distributions can be visualized in the pan-genome matrix. The pan-genome graph expresses every gene family and how they are ordered across all genomes, close-up examples of the graph are contained in Fig 3, S3-8. The interactive graph is found in Supplemental File S1 and can be visualized in Cytoscape (Shannon et al., 2003).

Querying the pan-genome graph for genomic islands

The pan-genome graph contains every single gene family in the pangenome (as nodes) and shows how each gene connects to the next (across all genomes) with its edges (which can be multifurcating). The graph itself was generated with the Panaroo pipeline, using –clean-mode strict and default parameters (Tonkin-Hill et al., 2020). The graph was traversed using the accessory script panaroo-gene-neighborhood, with –expand_no 20 and default parameters. This script was used for calculating the gene neighborhood paths for all 8,401 pan-genes, this provided the ±20 gene neighborhood for each gene. In this dataset, core genes have a representation of 44+ (in all genomes) and cloud genes have a representation in only one genome. The representation of all gene families (i.e., genome coverage or how many genomes a pan-gene is in) was overlayed onto the previously calculated gene neighborhood paths.

Genomic islands, by definition, cannot contain a core gene; but are often found invading between two core genes. These genomic islands always adhere to a simple representation pattern in this pan-genomic framework: core gene-(rare gene(s))-core gene. We searched the ±20 gene neighborhood paths (which now includes the representation of each gene) for the following coverage (representation) pattern: 44+-(1-43)x-44+, where x is ≥2. This returned any multi-gene fragment, of low coverage, that is contiguous with two flanking core genes (high coverage). The flanking core genes were retrieved for each insertion, and the adjacent island was visually inspected in the pangenome graph (final_graph.gml; File S1) in Cytoscape (Shannon et al., 2003). Only islands which contain few multifurcations and have a traceable path from one flanking core gene to the other was reported (50 total). Islands with complicated multifurcations, multiple core gene invasion, and divergent synteny were discarded (131 total). This approach provides a measure of reliability (i.e., coverage) by stipulating: 1) the inclusion of the invaded core genes (which has at least 95% coverage), and 2) the local synteny of the genomic island is intact (across all genomes which include the island). A hard-coded script of this search process can be found in the supplemental material as an interactive Jupyter Notebook (File S2).

Analysis of *Hez* population structure

The Tajima's D (Tajima, 1989) statistic was calculated for every core gene (i.e., a gene that is found in at least 44 of the 47 genomes) alignment using Pegas (Paradis, 2010), those gene families with a Tajima's D $<|0.2|$ were considered as not seen by purifying selection (i.e., almost neutral). Neutral core genes were concatenated and used to generate a SNP matrix. These genomes were hierarchically clustered, based on SNP distances,

into populations using RhierBAPs (Tonkin-Hill et al., 2018). The population membership for every genome was then mapped back to the tANI tree (Figure 1).

Inference of gene transfers

Proto-phylogenies (gene trees without correction applied) were calculated for all genes of interests and concatenates (islands). Proto-phylogenies, the associated nucleotide alignment, and the species tree (Figure 1) were supplied to treefixDTL (Wu et al., 2013) to produce the corrected phylogeny where HGT, topological information, and sequence likelihoods (probability of observing the sequences estimated using a pairwise distance matrix of the alignment under the JTT model) were considered. The corrected phylogenies were optimally rooted based on minimizing DTL reconciliation costs in OptRoot. These rooted phylogenies and the species tree were then supplied to RangerDTL2.0 (Bansal et al., 2018) where duplication, transfer, and loss events were inferred. Each gene tree in this analysis was explored through 300 independent runs in the reconciliation space using 3 different DTL costs ([2,3,1], [3,3,1], [2,4,1], costs for a [duplication, transfer, loss]). Inferred DTL events for each gene tree were normalized using the number of internal nodes and total branch length of the gene tree.

Identification of Restriction Modification Systems Genes

Query sequences for RMS genes were gathered using a slight modification of the method described by Fullmer et al., 2019. Briefly, all sequences on REBase were downloaded, and clustered using a 70% identity threshold in USearch. HMMs were built for all clusters and used to search the clustered gene families of the *Hez* pan-genome. Those gene families that matched an RMS gene, had their genomic neighborhood (5 genes upstream/downstream) searched for other RMS genes. RMS gene type assignment (Type 1-4) was determined by the best ReBase hit, and in the case of ambiguity for multiple RMS genes in the same neighborhood the assignment was typed using the restriction enzyme's annotation.

Author Contributions

The project was conceived by YF, ASL, and JPG. Sampling, sequencing, and genome assembly of the Israeli samples was conducted by N.A-P. and U.G., while A.S.L. and R.T.P was responsible for the Spanish and Iranian samples. D.A. and Y.F. performed the pan-genomic analyses. All authors contributed to the writing and editing of the manuscript.

Data Availability

New *Hez* draft genomes from Israel are found under BioProject PRJNA925523, and those genomes from Spain are found under BioProject PRJNA925515. Additionally, genome gff files, nucleotide sequences of island encoded genes, the pan-genome graph and additional supporting materials are deposited in supplemental_hezpg.zip..

Acknowledgements and Funding

This work was supported by grants from the Binational Science Foundation [BSF 2013061 to U.G., J.P.G., and R.T.P.]; the National Science Foundation [NSF/MCB 1716046 to U.G., R.T.P., and J.P.G.]. We thank Dr. Andrea Makkay for sequencing the Spanish strains. We also thank Dr. Anna Green for her insightful discussions of pan-genomics.

Conflict of Interest

The authors declare no conflict of interest.

References

Andam, C.P., Fournier, G.P., Gogarten, J.P., 2011. Multilevel populations and the evolution of antibiotic resistance through horizontal gene transfer. FEMS Microbiol. Rev. 35, 756–767. https://doi.org/10.1111/j.1574-6976.2011.00274.x

Andam, C.P., Gogarten, J.P., 2011. Biased gene transfer in microbial evolution. Nat. Rev. Microbiol. 9, 543–555. https://doi.org/10.1038/nrmicro2593

Andam, C.P., Williams, D., Gogarten, J.P., 2010. Biased gene transfer mimics patterns created through shared ancestry. Proc. Natl. Acad. Sci. 107, 10679–10684. https://doi.org/10.1073/pnas.1001418107

Bansal, M.S., Kellis, M., Kordi, M., Kundu, S., 2018. RANGER-DTL 2.0: rigorous reconstruction of gene-family evolution by duplication, transfer and loss. Bioinformatics 34, 3214–3216. https://doi.org/10.1093/bioinformatics/bty314

Bardavid, R.E., Oren, A., 2012. The amino acid composition of proteins from anaerobic halophilic bacteria of the order Halanaerobiales. Extremophiles. https://doi.org/10.1007/s00792-012-0455-y

Bertelli, C., Laird, M.R., Williams, K.P., Simon Fraser University Research Computing Group, Lau, B.Y., Hoad, G., Winsor, G.L., Brinkman, F.S.L., 2017. IslandViewer 4: expanded prediction of genomic islands for larger-scale datasets. Nucleic Acids Res. 45, W30–W35. https://doi.org/10.1093/nar/gkx343

Camargo, A.P., Roux, S., Schulz, F., Babinski, M., Xu, Y., Hu, B., Chain, P.S.G., Nayfach, S., Kyrpides, N.C., 2023. You can move, but you can't hide: identification of mobile genetic elements with geNomad. bioRxiv 2023.03.05.531206. https://doi.org/10.1101/2023.03.05.531206

Chen, K.Y., Martynowicz, H., 1984. Lack of detectable polyamines in an extremely halophilic bacterium. Biochem. Biophys. Res. Commun. 124, 423–429. https://doi.org/10.1016/0006-291X(84)91570-5

Clasen, F.J., Pierneef, R.E., Slippers, B., Reva, O., 2018. EuGI: a novel resource for studying genomic islands to facilitate horizontal gene transfer detection in eukaryotes. BMC Genomics 19, 323. https://doi.org/10.1186/s12864-018-4724-8

Coleman, M.L., Sullivan, M.B., Martiny, A.C., Steglich, C., Barry, K., DeLong, E.F., Chisholm, S.W., 2006. Genomic Islands and the Ecology and Evolution of Prochlorococcus. Science 311, 1768–1770. https://doi.org/10.1126/science.1122050

Corral, P., de la Haba, R.R., Infante-Domínguez, C., Sánchez-Porro, C., Amoozegar, M.A., Papke, R.T., Ventosa, A., 2018. Halorubrum chaoviator Mancinelli et al. 2009 is a later, heterotypic synonym of Halorubrum ezzemoulense Kharroub et al. 2006. Emended description of Halorubrum ezzemoulense Kharroub et al. 2006. Int. J. Syst. Evol. Microbiol. 68, 3657–3665. https://doi.org/10.1099/ijsem.0.003005

Cortez, D.Q., Lazcano, A., Becerra, A., 2005. Comparative analysis of methodologies for the detection of horizontally transferred genes: a reassessment of first-order Markov models. Silico Biol 5, 581–92.

Daubin, V., Szöllősi, G.J., 2016. Horizontal gene transfer and the history of life. Cold Spring Harb. Perspect. Biol. https://doi.org/10.1101/cshperspect.a018036

de la Haba, R.R., Corral, P., Sánchez-Porro, C., Infante-Domínguez, C., Makkay, A.M., Amoozegar, M.A., Ventosa, A., Papke, R.T., 2018. Genotypic and lipid analyses of strains from the archaeal genus Halorubrum reveal insights into their taxonomy, divergence, and population structure. Front. Microbiol. 9, 512.

Feng, Y., Louyakis, A.S., Makkay, A.M., Guerrero, R.O., Papke, R.T., Gogarten, J.P., 2019. Complete Genome Sequence of Halorubrum ezzemoulense Strain Fb21. Microbiol. Resour. Announc. https://doi.org/10.1128/mra.00096-19

Feng, Y., Neri, U., Gosselin, S., Louyakis, A.S., Papke, R.T., Gophna, U., Gogarten, J.P., 2021. The Evolutionary Origins of Extreme Halophilic Archaeal Lineages. Genome Biol. Evol. 13, evab166. https://doi.org/10.1093/gbe/evab166

Gal-Mor, O., Finlay, B.B., 2006. Pathogenicity islands: a molecular toolbox for bacterial virulence. Cell. Microbiol. 8, 1707–1719. https://doi.org/10.1111/j.1462-5822.2006.00794.x

Gauthier, C.H., Abad, L., Venbakkam, A.K., Malnak, J., Russell, D.A., Hatfull, G.F., 2022. DEPhT: a novel approach for efficient prophage discovery and precise extraction. Nucleic Acids Res. 50, e75–e75. https://doi.org/10.1093/nar/gkac273

Gogarten, J.P., Doolittle, W.F., Lawrence, J.G., 2002. Prokaryotic Evolution in Light of Gene Transfer. Mol. Biol. Evol. 19, 2226–2238. https://doi.org/10.1093/oxfordjournals.molbev.a004046

Gosselin, S., Fullmer, M.S., Gogarten, J.P., n.d. Expanding the utility of sequence comparisons using data from whole genomes.

Hacker, J., Carniel, E., 2001. Ecological fitness, genomic islands and bacterial pathogenicity: A Darwinian view of the evolution of microbes. EMBO Rep. https://doi.org/10.1093/embo-reports/kve097

, K., KAMEKURA, M., ONISHI, H., AKAZAWA, T., MATSUZAKI, S., 1985. Polyamines in Photosynthetic Eubacteria and Extreme-Halophilic Archaebacteria1. J. Biochem. (Tokyo) 97, 1653–1658. https://doi.org/10.1093/oxfordjournals.jbchem.a135223

Harms, C., Domoto, Y., Celik, C., Rahe, E., Stumpe, S., Schmid, R., Nakamura, T., Bakker, E.P., 2001. Identification of the ABC protein SapD as the subunit that confers ATP dependence to the K+-uptake systems TrkH and TrkG from Escherichia coli K-12. Microbiology 147, 2991–3003. https://doi.org/10.1099/00221287-147-11-2991

Huang, J., Gogarten, J.P., 2006. Ancient horizontal gene transfer can benefit phylogenetic reconstruction. Trends Genet. 22, 361–366. https://doi.org/10.1016/j.tig.2006.05.004

Huerta-Cepas, J., Szklarczyk, D., Heller, D., Hernández-Plaza, A., Forslund, S.K., Cook, H., Mende, D.R., Letunic, I., Rattei, T., Jensen, L.J., von Mering, C., Bork, P., 2019. eggNOG 5.0: a hierarchical, functionally and phylogenetically annotated orthology resource based on 5090 organisms and 2502 viruses. Nucleic Acids Res. 47, D309–D314. https://doi.org/10.1093/nar/gky1085

Johnson, H.A., Hampton, E., Lesley, S.A., 2009. The Thermotoga maritima Trk Potassium Transporter—from Frameshift to Function. J. Bacteriol. 191.

Juhas, M., van der Meer, J.R., Gaillard, M., Harding, R.M., Hood, D.W., Crook, D.W., 2009. Genomic islands: tools of bacterial horizontal gene transfer and evolution. FEMS Microbiol. Rev. 33, 376–393. https://doi.org/10.1111/j.1574-6976.2008.00136.x

Kamekura, M., Bardocz, S., Anderson, P., Wallace, R., Kushner, D.J., 1986. Polyamines in moderately and extremely halophilic bacteria. Biochim. Biophys. Acta BBA - Gen. Subj. 880, 204–208. https://doi.org/10.1016/0304-4165(86)90081-4

Kashiwagi, K., Innami, A., Zenda, R., Tomitori, H., Igarashi, K., 2002. The ATPase Activity and the Functional Domain of PotA, a Component of the Spermidine-preferential Uptake System inEscherichia coli *. J. Biol. Chem. 277, 24212–24219. https://doi.org/10.1074/jbc.M202849200

Katoh, K., Standley, D.M., 2013. MAFFT multiple sequence alignment software version 7: Improvements in performance and usability. Mol. Biol. Evol. https://doi.org/10.1093/molbev/mst010

Kharroub, K., Quesada, T., Ferrer, R., Fuentes, S., Aguilera, M., Boulahrouf, A., Ramos-Cormenzana, A., Monteoliva-Sánchez, M., 2006. Halorubrum ezzemmoulense sp. nov., a halophilic archaeon isolated from Ezzemoul sabkha, Algeria. Int. J. Syst. Evol. Microbiol. https://doi.org/10.1099/ijs.0.64272-0

Lawrence, J.G., Retchless, A.C., 2010. The myth of bacterial species and speciation. Biol. Philos. 25, 569–588. https://doi.org/10.1007/s10539-010-9215-5

Lee, S.-J., Surma, M., Seitz, S., Hausner, W., Thomm, M., Boos, W., 2007. Differential signal transduction via TrmB, a sugar sensing transcriptional repressor of Pyrococcus furiosus. Mol. Microbiol. 64, 1499–1505. https://doi.org/10.1111/j.1365-2958.2007.05737.x

Lu, B., Leong, H.W., 2016. Computational methods for predicting genomic islands in microbial genomes. Comput. Struct. Biotechnol. J. 14, 200–206. https://doi.org/10.1016/j.csbj.2016.05.001

Peck M.K., Lauring A.S., 2018. Complexities of Viral Mutation Rates. J. Virol. 92, e01031-17. https://doi.org/10.1128/JVI.01031-17

Makkay, A.M., Louyakis, A.S., Ram-Mohan, N., Gophna, U., Gogarten, J.P., Papke, R.T., 2020. Insights into gene expression changes under conditions that facilitate horizontal gene transfer (mating) of a model archaeon. Sci. Rep. 10, 22297. https://doi.org/10.1038/s41598-020-79296-w

Martínez-García, M., Santos, F., Moreno-Paz, M., Parro, V., Antón, J., 2014. Unveiling viral–host interactions within the 'microbial dark matter.' Nat. Commun. 5, 4542. https://doi.org/10.1038/ncomms5542

Mongodin, E.F., Nelson, K.E., Daugherty, S., DeBoy, R.T., Wister, J., Khouri, H., Weidman, J., Walsh, D.A., Papke, R.T., Perez, G.S., Sharma, A.K., Nesbø, C.L., MacLeod, D., Bapteste, E., Doolittle, W.F., Charlebois, R.L., Legault, B., Rodriguez-Valera, F., 2005. The genome of Salinibacter ruber: Convergence and gene exchange among hyperhalophilic bacteria and archaea. Proc. Natl. Acad. Sci. U. S. A. https://doi.org/10.1073/pnas.0509073102

Naor, A., Altman-Price, N., Soucy, S.M., Green, A.G., Mitiagina, Y., Turgeman-Grotta, I., Davidovich, N., Gogarten, J.P., Gophna, U., 2016. Impact of a homing intein on recombination frequency and organismal fitness. Proc. Natl. Acad. Sci. U. S. A. https://doi.org/10.1073/pnas.1606416113

Naor, A., Lapierre, P., Mevarech, M., Papke, R.T., Gophna, U., 2012. Low species barriers in halophilic archaea and the formation of recombinant hybrids. Curr. Biol. https://doi.org/10.1016/j.cub.2012.05.056

Nelson, K.E., Clayton, R.A., Gill, S.R., Gwinn, M.L., Dodson, R.J., Haft, D.H., Hickey, E.K., Peterson, J.D., Nelson, W.C., Ketchum, K.A., McDonald, L., Utterback, T.R., Malek, J.A., Linher, K.D., Garrett, M.M., Stewart, A.M., Cotton, M.D., Pratt, M.S., Phillips, C.A., Richardson, D., Heidelberg, J., Sutton, G.G., Fleischmann, R.D., Eisen, J.A., White, O., Salzberg, S.L., Smith, H.O., Venter, J.C., Fraser, C.M., 1999. Evidence for lateral gene transfer between Archaea and Bacteria from genome sequence of Thermotoga maritima. Nature 399, 323–329. https://doi.org/10.1038/20601

Oren, A., 2008. Microbial life at high salt concentrations: Phylogenetic and metabolic diversity. Saline Syst. https://doi.org/10.1186/1746-1448-4-2

Papke, R.T., Corral, P., Ram-Mohan, N., Haba, R.R. de la, Sánchez-Porro, C., Makkay, A., Ventosa, A., 2015. Horizontal Gene Transfer, Dispersal and Haloarchaeal Speciation. Life 5, 1405–1426. https://doi.org/10.3390/life5021405

Paradis, E., 2010. pegas: an R package for population genetics with an integrated–modular approach. Bioinformatics 26, 419–420. https://doi.org/10.1093/bioinformatics/btp696

Parks, D.H., Imelfort, M., Skennerton, C.T., Hugenholtz, P., Tyson, G.W., 2015. CheckM: Assessing the quality of microbial genomes recovered from isolates, single cells, and metagenomes. Genome Res. https://doi.org/10.1101/gr.186072.114

Pearson, S., 2022. Experimental Analysis of Genes Important for Amino Acid and Extracellular DNA Metabolism. UCONN PhD Diss.

Prunetti, L., Graf, M., Blaby, I.K., Peil, L., Makkay, A.M., Starosta, A.L., Papke, R.T., Oshima, T., Wilson, D.N., de Crécy-Lagard, V., 2016. Deciphering the Translation Initiation Factor 5A Modification Pathway in Halophilic Archaea. Archaea 2016, 7316725. https://doi.org/10.1155/2016/7316725

Ragan, M.A., 2001. On surrogate methods for detecting lateral gene transfer. FEMS Microbiol Lett 201, 187–91.

Makarova K.S., Wolf Y.I., Snir, S., Koonin E.V., 2011. Defense Islands in Bacterial and Archaeal Genomes and Prediction of Novel Defense Systems. J. Bacteriol. 193, 6039–6056. https://doi.org/10.1128/JB.05535-11

Seemann, T., 2014. Prokka: Rapid prokaryotic genome annotation. Bioinformatics. https://doi.org/10.1093/bioinformatics/btu153

Shannon, P., Markiel, A., Ozier, O., Baliga, N.S., Wang, J.T., Ramage, D., Amin, N., Schwikowski, B., Ideker, T., 2003. Cytoscape: A Software Environment for Integrated Models of Biomolecular Interaction Networks. Genome Res. 13, 2498–2504.

Sharma, A.K., Walsh, D.A., Bapteste, E., Rodriguez-Valera, F., Ford Doolittle, W., Papke, R.T., 2007. Evolution of rhodopsin ion pumps in haloarchaea. BMC Evol. Biol. https://doi.org/10.1186/1471-2148-7-79

Soucy, S.M., Fullmer, M.S., Thane Papke, R., Gogarten, J.P., 2014. Inteins as indicators of gene flow in the halobacteria. Front. Microbiol. https://doi.org/10.3389/fmicb.2014.00299

Tajima, F., 1989. Statistical method for testing the neutral mutation hypothesis by DNA polymorphism. Genetics 123, 585–595. https://doi.org/10.1093/genetics/123.3.585

Tonkin-Hill, G., Lees, J.A., Bentley, S.D., Frost, S.D.W., Corander, J., 2018. RhierBAPS: An R implementation of the population clustering algorithm hierBAPS. Wellcome Open Res. 3, 93. https://doi.org/10.12688/wellcomeopenres.14694.1

Tonkin-Hill, G., MacAlasdair, N., Ruis, C., Weimann, A., Horesh, G., Lees, J.A., Gladstone, R.A., Lo, S., Beaudoin, C., Floto, R.A., Frost, S.D.W., Corander, J., Bentley, S.D., Parkhill, J., 2020. Producing polished prokaryotic pangenomes with the Panaroo pipeline. Genome Biol. 21, 180. https://doi.org/10.1186/s13059-020-02090-4

Tschitschko, B., Erdmann, S., DeMaere, M.Z., Roux, S., Panwar, P., Allen, M.A., Williams, T.J., Brazendale, S., Hancock, A.M., Eloe-Fadrosh, E.A., Cavicchioli, R., 2018. Genomic variation and biogeography of Antarctic haloarchaea. Microbiome 6, 113. https://doi.org/10.1186/s40168-018-0495-3

Williams, D., Gogarten, J.P., Papke, R.T., 2012. Quantifying homologous replacement of loci between haloarchaeal species. Genome Biol. Evol. https://doi.org/10.1093/gbe/evs098

Williams, K.P., 2002. Integration sites for genetic elements in prokaryotic tRNA and tmRNA genes: sublocation preference of integrase subfamilies. Nucleic Acids Res. 30, 866–875. https://doi.org/10.1093/nar/30.4.866

Wu, Y.-C., Rasmussen, M.D., Bansal, M.S., Kellis, M., 2013. TreeFix: Statistically Informed Gene Tree Error Correction Using Species Trees. Syst. Biol. 62, 110–120. https://doi.org/10.1093/sysbio/sys076

Zimmermann, L., Stephens, A., Nam, S.-Z., Rau, D., Kübler, J., Lozajic, M., Gabler, F., Söding, J., Lupas, A.N., Alva, V., 2018. A Completely Reimplemented MPI Bioinformatics Toolkit with a New HHpred Server at its Core. J. Mol. Biol. 430, 2237–2243. https://doi.org/10.1016/j.jmb.2017.12.007

Supplemental Material Table of Contents

Figures

Figure S1. **A description of the *Halorubrum ezzemoulense* pan-genome calculated by Panaroo.**

Figure S2. **2,621 core genes phylogeny of *Hez* isolates.**

Figure S3. **RMS distribution mapped onto phylogeny**.

Figure S4. **Pan-genome graph close up of Islands 4+5.**

Figure S5. **Pan-genome graph of Islands 13+14.**

Figure S6. **Pan-genomic graph of Islands 23+24.**

Figure S7. **Pan-genome graph of Islands 27+28.**

Figure S8. **Pan-genome graph of Islands 42+43**.

Figure S9. **Depiction of islands 44 and 45.**

Figure S10. **Variations of the *dppDF* transporters contained on the islands of *Hez.***

Figure S11. **Comparison of *phnCDE* genes in *Halorubrum ezzemoulense* and *Haloferax volcanii.***

Spreadsheets

Spreadsheet S1. **Information of assembled genomes from isolates.**

Spreadsheet S2. **Pairwise tANI distance matrix.**

Spreadsheet S3. **Description of Gene Content Encoded on Islands.**

Spreadsheet S4. **Information on integrase containing islands.**

Spreadsheet S5. **Reports of island encoded restriction modification system genes.**

Spreadsheet S6. **Inferred DTL events for islands and core genes.**

Spreadsheet S7. **Description of transposable elements found within the proximity of islands.**

Spreadsheet S8. **Homeoallele searches between opposing islands.**

Spreadsheet S9. **Descriptions of transporter encoding islands.**

Spreadsheet S10. **Investigation of AMM015's competitive genomic islands.**

Supplemental Discussion

Restriction modification systems

AMM015 – a strain that harbors both islands of a conflicting pair

The only *Hez* CUT transporter is encoded on a rare island

Island encoded transporters reveal a polyamine scavenging mechanism

Variations of Trk-type K+ import encoded on a homeocassette

Divergent di/oligopeptide transporters are retained in the *Hez* pan-genome on islands

The island encoded phosphate transporter is a variation of a homologous core gene neighborhood

Supplemental Files

File S1. **Pan-genome graph.** final_graph.gml

File S2. **Jupyter notebook of island search process.** find_islands.ipynb

File S3. **Island gene alignments.** Island_gene_seqs.zip